HHS Public Access

Author manuscript

*Retina*. Author manuscript; available in PMC 2017 November 01.

Published in final edited form as:

*Retina*. 2016 November ; 36(11): 2039–2050. doi:10.1097/IAE.0000000000001077.

# Characterization of the Middle Capillary Plexus Using Optical Coherence Tomography Angiography in Healthy and Diabetic Eyes

**JUSTIN J. PARK, BS**[1], **BRIAN T. SOETIKNO, BS**[1,2,3], and **AMANI A. FAWZI, MD**[1]

[1]Department of Ophthalmology, Feinberg School of Medicine, Northwestern University, Chicago, Illinois

[2]Functional Optical Imaging Laboratory, Department of Biomedical Engineering, Northwestern University

[3]Medical Scientist Training Program, Northwestern University Feinberg School of Medicine, Chicago, IL

## Abstract

**Purpose—**To assess the ability of optical coherence tomography angiography (OCTA) to image the retinal middle capillary plexus (MCP), and to characterize the MCP as a unique vascular network separate from the superficial (SCP) and deep capillary plexus (DCP).

**Methods—**Healthy and diabetic eyes were imaged using the Avanti XR OCTA instrument (Optovue Inc, Fremont, California, USA). Using manual segmentation of the retinal layers, we generated *en face* angiograms to distinguish the three capillary plexuses (SCP, MCP, DCP).

**Results—**In healthy eyes, arterioles gave rise to distinct branches in the MCP, and venules gave rise to prominent vortex like branches in the DCP. The foveal avascular zone (FAZ) was most well-defined at the level of the MCP, and had a larger area in the DCP. In diabetic eyes, the three capillary plexuses showed varying degrees of non-perfusion, including variable shapes and extent of the FAZ, with loss of border integrity at the MCP. Microaneurysms appeared in all of the three capillary plexuses.

**Conclusions—**Using customized segmentation analysis in OCTA, we demonstrate that the MCP is qualitatively and functionally distinct from the SCP and DCP, which may help clarify the pathogenesis of different middle retinal ischemic entities and provide new insights into retinal ischemia in diabetic retinopathy.

Corresponding author: Amani Fawzi, MD; Department of Ophthalmology, Feinberg School of Medicine, Northwestern University, 645 N. Michigan Avenue, Suite 440, Chicago, IL 60611, USA; afawzimd@gmail.com; Tel: +1 (312) 908 8152; Fax: 312-503-8152.

Study site institution: Department of Ophthalmology, Feinberg School of Medicine, Northwestern University, Chicago, Illinois

Conflict of Interest: No conflicting relationship exists for any author.

Proprietary interest: The authors have no proprietary interest in the subject of this manuscript

Summary statement: Using manual segmentation and artifact removal software in optical coherence tomography angiography, we show the middle retinal capillary plexus as a distinct vascular network, providing novel insights into the study of retinal vasculature.

**Keywords**

Capillary plexus; Diabetic retinopathy; OCT Angiography

## Introduction

Optical coherence tomography angiography (OCTA) is a recently developed, non-invasive, dye-less imaging modality, which can visualize moving blood within retinal vessels. Clinical studies of retinal vasculature have long relied upon fluorescein angiography (FA) to provide important details about the retinal microvasculature. However, the injected fluorescein carries well-documented side effects,[1] and FA images are two dimensional and thus unable to adequately visualize the deeper retinal networks. For example, in an FA study of non-human primate retina, Weinhaus et al. found that superficial capillaries were visualized more than four times as effectively as comparable capillaries in the deepest vascular plane, obfuscating the majority of the multilaminar network adjacent to the FAZ.[2]

The major advantage of OCTA, then, is its ability to resolve the vascular layers of the retina in three-dimensions.[3] With this capability, the majority of software analysis tools for OCTA have separated the inner retinal capillaries into two plexuses: a superficial capillary plexus (SCP) and a deep capillary plexus (DCP). However, there is significant evidence from anatomical and developmental studies that a third capillary plexus exists, the middle capillary plexus (MCP), which is generally not revealed in current OCTA software that incorporates segments of the MCP into either the SCP or DCP angiograms.

Histological studies in humans [4] have consistently identified four planes of capillaries in the central retina surrounding the fovea. Around the macula, these capillary planes form three layers: the SCP, the MCP, and the DCP. The MCP lies at the inner boundary of the INL, while the DCP lies at the deep boundary between the inner nuclear layer (INL) and outer plexiform layer (OPL). The SCP lies at the level of the retinal nerve fibers, which is the same level as the major arterioles and venules. Around the optic nerve, an additional fourth, more superficial capillary network, the radial peripapillary capillaries, exists.[5-7]

In addition to being anatomically distinct from the SCP and DCP, the development of primate retinal vasculature also shows that the MCP is a unique entity. The sequence of development of the perifoveal capillary beds around the foveal avascular zone (FAZ) occurs in three phases of development. First, beginning at fetal day 105, capillaries in the ganglion cell layer, guided by a grid network of astrocytes, grow towards the fovea and define the location of FAZ. Second, five to six weeks later, downward sprouting of these superficial capillaries establishes the deep plexus at the outer border of the INL[8]. Third, during the perinatal period, upwards sprouting from the DCP establishes the MCP at the inner border of the INL, driven by angiogenic stimuli from the amacrine cells.[9] The foveal pit is established with maturation of the MCP network, in conjunction with lateral migration of the Henle fiber layer, while anastomoses between the three networks around the FAZ occur post-natally.[8]

Distinguishing the MCP from the SCP and DCP is not only important from a scientific point of view, but may also be important from a clinical standpoint. In diabetic retinopathy, for example, macular ischemia and enlargement of the foveal avascular zone can differentially affect the DCP. [10, 11] Moreover, disorganization of the retinal inner layers (DRIL)[12] and paracentral acute middle maculopathy (PAMM)[13], which commonly occur in diabetic retinopathy, are likely manifestations of ischemia at the level of the SCP and MCP, respectively. More importantly, we have recently shown that diabetic capillary non-perfusion can be associated with photoreceptor and outer retinal disruption on OCT, which could be a specific manifestation of non-perfusion at the DCP (in review).[14] Therefore, imaging of the distinct capillary networks can shed important light on these complex and multilaminar manifestations of macular ischemia, as they may relate to corresponding capillary networks.

The goal of the current study was to explore whether OCTA could distinguish the three different capillary plexuses, as the current OCTA segmentation software artificially splits the retinal capillaries into two networks rather than three, as would be expected anatomically. In this study, we used manual segmentation to visualize the three capillary plexus *en face* angiograms. We then used software to remove projection artifacts from the angiograms and combined them into a composite pseudo-color image for improved visualization. Our study identified reliable and repeatable segmentation boundaries, whereby the three unique capillary plexuses can be successfully visualized in both healthy and diabetic eyes.

## Methods

The institutional review board at Northwestern University approved this prospective observational study; informed consent was obtained from all subjects. This study followed the tenets of the Declaration of Helsinki and was HIPAA-compliant. We prospectively collected imaging data on subjects examined at the Department of Ophthalmology, Feinberg School of Medicine of Northwestern University, Chicago, Illinois. Healthy control subjects without a history of diabetes were recruited from the optometry practice, while patients with various stages of diabetic retinopathy were recruited from the retina practice. Inclusion criteria for healthy controls included subjects between the ages of 20 and 80 with no prior history of ophthalmologic disease other than corrected refractive error, and for diabetic patients, inclusion criteria included patients diagnosed with diabetic retinopathy ranging from non-proliferative to proliferative diabetic retinopathy. Exclusion criteria for this study included patients with any significant media opacity or cataracts that generated artifacts or produced poor image quality.

Images were obtained using the RTVue XR Avanti OCTA instrument (Optovue Inc, Fremont, California, USA), which uses the split-spectrum amplitude-decorrelation angiography (SSADA) algorithm in its software.[3] This instrument has an A-scan rate of 70,000 scans per second and uses a light source centered on 840 nm and a bandwidth of 45 nm. To produce three-dimensional angiograms, two consecutive OCT volumes (containing 304 B-scans with 304 A-lines per B-scan) were acquired in a 3 × 3 mm scanning area centered on the fovea and the SSADA algorithm was applied.

### Segmentation of the Three Capillary Plexuses

In order to define the three different capillary networks to produce angiograms, layers within the OCT volumes were manually segmented according to three different methods (Methods 1-3), in order to determine the most effective way to visualize three distinct networks.

**Method 1** (Supplemental Digital Content 1, Figure 1): We used the boundaries for the SCP and DCP as automatically pre-set by the built-in software. For the SCP, the inner boundary of the en face image segment was set at 3 μm beneath the internal limiting membrane (ILM), and the outer boundary was set at 15 μm beneath the inner plexiform layer (IPL) (Supplementary Figure 1A). For the DCP, the inner boundary of the en face image segment was set at 15 μm beneath the IPL and the outer boundary was set at 70 μm beneath the IPL (Supplementary Figure 1C). The MCP was set by first adjusting the boundaries of the DCP setting in order to create a thin slab. To do this, the inner boundary was kept at 15 μm beneath the IPL while the outer boundary was moved from 70 to 30 μm beneath the IPL, creating a thin 15 μm slab that could then be moved to rest at the inner border of the INL (Supplementary Figure 1B).

**Method 2 (**Supplemental Digital Content 2, Figure 2): Here we manually set the boundaries for the SCP and DCP according to their known anatomical location. Based on confocal imaging of human retinal microvasculature, the SCP is located in the nerve fiber layer (NFL) and ganglion cell layer (GCL), the MCP is located at the outer border of the inner plexiform layer (IPL) and superficial boundary of the INL, and the DCP is located at the boundary between the deep INL and outer plexiform layer (OPL).[15] Using these anatomical guidelines, the SCP boundaries were set by keeping its inner boundary set at the automated level of 3 μm beneath the ILM, while moving the outer boundary inward to create a thinner slice sufficient to incorporate the NFL and GCL while not encroaching onto the inner border of the INL (Supplementary Figure 2A). The DCP boundaries were set by first creating a thin slice and moving the slice to the outer border of the INL. This slice was created by starting at the automated boundaries for the DCP, keeping the inner boundary at 15 μm beneath the IPL while the outer boundary was moved from 70 to 30 μm beneath the IPL, creating a thinner 15μm slab that was then moved to rest at the outer border of the INL (Supplementary Figure 2C). The MCP was set in the same way as described in Method 1 (Supplementary Figure 2B).

**Method 3** (Figure 1): Here we capitalized on a recently recognized artifact within the en face angiograms, where capillaries are more clearly seen when reflected on the retinal layer just external to their location, and thus may be best visualized by focusing the segmentation onto the anatomic layer immediately external to them.[16] Furthermore, *ex vivo* quantitative confocal imaging of human retinal microvasculature show that the capillaries in the GCL (SCP) and at the superficial boundary of the INL (MCP) display a more three-dimensional configuration, while the capillaries in the deepest capillary network (DCP) demonstrate a laminar configuration projecting along a single plane.[15] The SCP boundaries were thus widened from those used in Method 2 to encompass the NFL, GCL and IPL by keeping the internal boundary at 3 μm beneath the ILM and setting the outer boundary at an offset of 25 μm above the preset IPL, in order to sufficiently capture the entire IPL while not

encroaching upon the INL (Figure 1A). The MCP boundaries were also widened from those used in the first two methods by creating a 30 μm slab and placing the slab to capture the entire INL, setting the boundaries at the border between the IPL and INL (0 μm offset from IPL setting) and 30 μm beneath the IPL (Figure 1B). Finally, the DCP was set by using a thin 15 μm slab and setting it below the INL to capture the entire OPL, with boundaries resting at 45 and 60 μm beneath the IPL (Figure 1C)

### Composite Color-coded Angiograms of The Three Capillary Networks and removal of vascular projection artifact

We developed a simple method to simultaneously display the three capillary plexuses with high contrast in a composite color image. The goal was to remove the vessel shadowing artifacts in OCTA, where vessels located at a more superficial level project onto the angiograms at a deeper capillary layer.[17] For example, a large vessel in the SCP angiogram may still appear in the DCP angiogram. Therefore, we produced composite images in two sequential steps: subtraction and color merging. First, we performed image subtraction to remove shadowing artifacts. The subtraction process can be mathematically written as:

$$\mathrm{I_S}\,(\mathrm{x},\mathrm{y}) = \mathrm{I_1}\,(\mathrm{x},\mathrm{y}) - \alpha I_2\,(\mathrm{x},\mathrm{y})$$

where $I_S(x,y)$ is the pixel in the final subtracted angiogram image; $I_1(x,y)$ is a pixel in a relatively deeper layer; and $I_2(x,y)$ is a pixel in a relatively more superficial layer. The parameter $\alpha$ controls the magnitude of subtraction between the two images and can be adjusted manually, albeit in a time consuming manner. We used a systematic approach to choose the best $\alpha$, by thresholding $I_1$ using Otsu's method (MATLAB, R2015b, MathWorks), which yielded a set S of the pixels representing the major vessels in the more superficial angiogram. We then iteratively increased $\alpha$ until 80% of the pixels in S were negative in the final image $I_S$. The negative values were then set to zero, and the final subtracted angiogram was saved. This subtraction process was only performed on the MCP and DCP angiograms, which were subtracted by the SCP and MCP angiograms, respectively. After the subtraction process, we merged the SCP angiogram with the subtracted MCP and DCP angiograms in Fiji (National Institutes of Health, Bethesda, MD, USA), using the "Color > Merge Channels" feature. The SCP was assigned the color yellow; the MCP cyan; and the DCP magenta. Images of the three capillary plexuses and composite were used for qualitative and descriptive analysis to identify patterns and differences between the three different capillary plexuses (see Composite columns in Figures 2-5). The entire procedure was performed manually: we performed manual segmentation, subtraction of projection artifact to color assignment and then created the color-coded maps. The process took on average less than ten minutes for each eye analyzed. However, with automated analysis and batch software processing, we believe this could be much faster.

## Results

This study included ten eyes of ten healthy volunteers, and twelve eyes of nine patients diagnosed with various stages of diabetic retinopathy. The demographic characteristics of

the healthy controls are summarized in Supplemental Digital Content 3 (Table 1), and for the diabetic patients in Supplemental Digital Content 4 (Table 2).

We found that *Method 3* was the most effective in distinguishing the three capillary networks, and used it for analysis of all eyes in this study. We found that the segmentation guidelines were effective in healthy and diseased eyes, and required no additional adjustments when applied to diseased eyes. However, in cases of severe retinal tissue reduction due to atrophy or edema, the segmentation contour could be affected and therefore the planes suggested for segmentation in Method 3 may not apply and may have to be altered appropriately.

## Healthy Eyes

Qualitative analysis of the capillary plexuses in healthy eyes revealed several patterns. In the superficial plexus, we could distinguish arterioles from venules by their wider capillary-free zone.[18] We labeled arterioles (red A) and venules (blue V) in Figure 2A, and circled their branches (red for arterioles, blue for venules) in each of the three plexuses. Tracing the branches of the larger arterioles and venules into the deeper capillary plexuses, as shown by the yellow paths in Figure 2B, we found that arterioles had distinct branches in the MCP, while venules arose from prominent vortex like collecting channels at the DCP, as depicted by the red and blue circles in Figure 2C.

We also observed several interesting differences regarding the FAZ across the three capillary networks. In all eyes, the FAZ was best distinguished at the MCP as having a well-demarcated and clearly circumscribed border, with contributions arising from both arterioles and venules, labeled again with red A for arterioles and blue V for venules in Figure 3A, forming a well-defined and continuous capillary ring (Figure 3B). Furthermore, the overlap between MCP and DCP observed in composite angiograms was not present around the FAZ in the parafoveal region, as the DCP did not extend as close to the FAZ border as the MCP (Figure 3C). This can be best appreciated in the composite images where the cyan vessels of the MCP can be seen bordering the FAZ while the magenta vessels of the DCP are distant from the FAZ, without having an intimate relationship to the FAZ (Figure 3D). Consequently, we observed that the FAZ is distinctly larger and less well defined in the DCP compared to the MCP (Figure 3).

## Diabetic Eyes

In diabetic eyes, qualitative analysis showed that the three capillary plexuses had non-overlapping zones of non-perfusion, including varying shapes and extent of the FAZ. For example, the FAZ in the DCP was observed to extend over a greater area than the MCP (Figures 4B,C). Interestingly, the well-demarcated border of the FAZ seen in healthy eyes at the level of the MCP was completely absent in diabetic eyes, with multiple breaks and gaps in the FAZ at the MCP (Figure 4B). Furthermore, the significant overlap of the capillary layers observed in composite images of healthy eyes was markedly reduced in diabetic eyes, where many retinal locations had a single capillary plexus. This can be best appreciated in composite images, where areas of distinct yellow (SCP), cyan (MCP) and magenta (DCP) can be observed (Figure 4D).

Microaneurysms, which were identified as areas of focally dilated, round, saccular or fusiform capillaries,[11] could also be seen across the three capillary plexuses (Figure 5A,B,C). As depicted by the yellow arrows in Figure 5A and Figure 5B, multiple microaneurysms can be seen in both the SCP and MCP layers, respectively. Figure 5C shows that there were few microaneurysms in the DCP.

A summary of the major morphological characteristics observed across the three capillary plexuses in healthy and diabetic eyes is provided in Table 1.

## Discussion

Using customized manual segmentation, we have successfully used OCTA to distinguish the MCP as a unique network, separate from the SCP and DCP in healthy eyes and eyes with diabetic retinopathy. Current pre-set automated segmentation software in the Optovue OCTA system divides the capillary plexuses into two at the middle of the INL. Therefore, components of the MCP are incorporated into the SCP (mainly) and the DCP. By customizing the segmentation boundaries to separate the MCP from the SCP and DCP, our study identified unique characteristics of the MCP in healthy and diabetic eyes.

### Healthy Eyes

Analysis of healthy eyes in our study revealed different branching patterns of arterioles and venules involving the MCP. We show that retinal arterioles continue into the MCP to give rise to capillary branches before proceeding to the DCP (Figure 2B), while capillary tangles at the level of the DCP, appearing as spider-web vortices, first described by Savastano et al.[19], likely drain directly into the superficial venules (Figure 2C). These DCP findings are consistent with other recent studies using OCTA. Bonnin et al. similarly used OCTA to characterize the deep plexus and showed deep capillary vortices as radial convergences of capillaries toward an epicenter aligned along the course of macular venules. However, to segment the DCP in this study, the authors used the preset segmentation provided by the vendor software (15 and 70 μm beneath the IPL), then further isolated the vortices to the DCP using customized segmentation. When a 20 μm slab was placed at 50 and 70 μm beneath the IPL, the capillary vortex pattern became visible.[20] This segmentation approach agrees with our method to identify the DCP between 45 and 60 μm beneath the IPL, where the capillary vortices in the DCP are located. While they did not separately evaluate the MCP, characterization of retinal vascular morphology with OCTA by Savastano et al. also support our image findings, though their conclusions are slightly different. These authors confirmed that the SCP is located in the GCL and the DCP in the OPL. Moreover, they showed, by moving through a sequenced stack of OCTA *en face* angiograms from superficial to deep, that there is a persistence of flow, indicating capillary interconnections between the SCP and DCP, but these authors were not able to detect the specific MCP network.[19] To complement these findings, our results confirm that arterioles from the SCP branch in the MCP before entering the DCP, which likely correspond to their finding of continuous flow. In addition we were able to distinguish these connections as a distinct capillary network in MCP (Figure 2A,B).

Our findings are also consistent with functional distribution of the macular capillaries in rodent retinal vasculature. Following transient branch retinal vein occlusion in rats, Genevois et al. reported that the three retinal capillary networks (particularly the MCP) were differentially affected by capillary closure. These authors found that the MCP was functionally predominantly arterial, while the dense capillary plexus of the DCP is largely consistent of postcapillary venules that eventually join major venules in the SCP.[21]

Our study also suggests that the FAZ may be more distinct in the MCP as a well-defined avascular zone surrounded with an intact ring of inter-connected capillaries arising from both arterioles and venules (Figure 3B). This finding is consistent with histological study of primate retinal vasculature that shows the FAZ is surrounded by capillary networks interconnecting in a radial array of alternating arteries and veins,[5, 6] and that during infancy, vessels circumscribing the fovea anastomose to form a continuous capillary border.[22] This particular arrangement of the FAZ with a continuous capillary border was only seen in our study in the MCP angiogram. The FAZ has also been recently characterized using OCTA by Samara et al., showing that the FAZ area is significantly larger in the DCP than the SCP.[23] However, this study used automatic pre-set segmentation from vendor software to define the SCP and DCP and, thus, did not account for the morphology of the FAZ in the MCP. In our healthy controls, the FAZ had the smallest diameter at the MCP, appearing larger at the SCP and DCP. The difference between our results and these authors relates to the fact that the MCP is largely incorporated in the SCP angiograms in current software, which may explain these authors' finding of smaller size of FAZ in SCP.

The larger size of the FAZ at the DCP (Figure 3C) compared to the MCP (Figure 3B) is intriguing. One might hypothesize that variations in capillary distribution and density may confer individual susceptibility to vascular middle retinal ischemic disease states, such as acute macular neuroretinopathy (AMN) and paracentral acute middle maculopathy (PAMM). Since we did not perform quantitative measurements of the FAZ or vascular density at the different levels, this would be an area of important future study.

## Diabetic Eyes

The study of OCTA in diabetic retinopathy by Ishibazawa et al. and Couturier et al. both showed that areas of non-perfusion were significantly larger in the SCP compared to the DCP.[11,24] However, in both these studies, the automatically determined layer boundaries from vendor software were used to segment the SCP and DCP. Compared to these authors, our analysis shows that the areas of non-perfusion differ qualitatively across the three plexuses, and areas of nonperfusion in the MCP may be contributing to differences observed in these studies (Figure 4). Similarly, Takase et al. used OCTA to analyze the FAZ in diabetic patients, and showed that diabetic eyes had significantly enlarged FAZ compared with healthy eyes.[25] However, when analyzing the FAZ in diabetic patients, this study also used the pre-set automated boundaries to characterize the FAZ in the SCP and DCP. Our analysis in diabetic eyes shows that the FAZ varies across the three capillary plexus layers, with a noticeably larger FAZ in the DCP when compared to the MCP (Figure 4C vs. Figure 4B). In addition, we observed an apparent loss of FAZ border integrity in the MCP (Figure 4B). Differences in FAZ size across the SCP and DCP in these previous studies may be

influenced by FAZ changes in the MCP, which is currently integrated partially into the SCP and DCP images.

Retinal capillary responsiveness to hypoxic retinal neurons begins during retinal development, where retinal neuronal maturation and their increasing neural metabolic demands directly stimulate retinal vascular development. The development of the SCP is closely associated with ganglion cell metabolic needs, signaled through the astrocytes, which lay the template for the advancing endothelial cell. These astrocytes are acutely sensitive to hypoxia, and their position, a few hundred microns ahead of the growing front of the developing retinal vascular endothelium allows them to sense hypoxia and guide the vascular network into the avascular retina.[8] In turn, development of the MCP is driven by INL hypoxia, signaled through the amacrine cells, as recently shown by elegant rodent studies. These genetic ablation studies confirmed that vascular endothelial growth factor (VEGF) signaling in amacrine cells plays a key role in regulating the development and capillary density of the MCP. More interestingly, these authors showed that ablation of VEGF in the amacrine cells in adult mice can lead to regression of the MCP, which may have important implications in understanding the neurovascular pathophysiology of ischemia of the middle retina.[9] Interestingly, global knockout of hypoxia-inducible factor 1A (HIF-1A) in mice leads to preferential attenuation of the MCP. As VEGF gene expression is primarily regulated by HIFs, this finding further supports the MCP as a developmentally distinct capillary plexus that is exquisitely sensitive and differentially regulated in hypoxia.[26] Thus, retinal non-perfusion at the MCP may have distinct and specific implications, related to INL ischemia and amacrine cell compromise, as compared to SCP or DCP ischemia.

This exquisite sensitivity of the MCP hypoxia may explain histolopathologic and OCT evidence that microaneurysms preferentially cluster in the INL in diabetic retinopathy.[27-29] Two recent OCTA studies showed that microaneurysms are more often found in the DCP than in the SCP.[11, 24] It will be important to reassess these findings as they relate to the MCP, since these studies have used the preset, INL-splitting segmentation boundaries to study the location of microaneurysms. In contrast, our analysis shows that microaneurysms are seen in the MCP as well as the DCP (Figure 5B,C), which may be an important distinction, as the MCP and DCP bracket the inner and outer borders of the INL. This corresponds with a histological study by Tan et al. that shows microaneurysms can be observed in each of the four retinal capillary layers,[30] further highlighting the importance of distinguishing the MCP separately from the SCP and DCP.

## Further Clinical Implication in Acute Macular Neuroretinopathy and Paracentral Acute Middle Maculopathy

The application of OCTA for the visualization of the MCP may have significant clinical implications in assessment of AMN and PAMM. AMN was originally characterized by Bos and Deutman as dark, wedge-shaped intraretinal lesions pointing to the fovea and sparing the retinal pigment epithelium (RPE) in women using oral contraceptives.[31] Recent multimodal imaging of AMN showed that acute changes in AMN begin at the level of the ONL and the OPL causing transient hyperreflectivity of these layers on OCT, followed by characteristic sequential disruption of the photoreceptors,. Long-term thinning of ONL,

outer segments and disruption of the interdigitation zone on OCT were residual hallmarks of this condition.[32] Based on this sequence, we originally hypothesized that AMN is caused by ischemia at the DCP, which would explain the disease course, the recently identified associated ischemic conditions [33] and long term thinning of ONL and photoreceptors. [32]

More recently, another ischemic injury of the middle retina at the level of the INL was termed PAMM.[34] PAMM lesions were originally proposed to be the result of ischemia of the SCP,[34] but consideration of the anatomical location of the MCP immediately superficial to PAMM lesions suggests more likely involvement of this plexus.[35] Further emphasizing the importance of improved segmentation of MCP, recent case studies of PAMM imaged using OCTA have demonstrated attenuated blood flow of the DCP.[36] However, the difficulty in distinguishing the DCP from the MCP using current software in OCTA as well as significant projection artifacts could complicate any OCTA study of retinal capillary involvement in PAMM and AMN. Thus, defining the exact level of capillary ischemia in PAMM and AMN, as related to the MCP and/or DCP respectively, would benefit greatly from improved OCTA segmentation and removal vascular projection artifact to accurately separate the MCP and DCP.

### Conclusion

In summary, using customized manual segmentation and software to remove projection artifact, we were able to generate *en face* angiograms that distinguish the SCP, MCP and DCP. Our study demonstrates that the MCP is a qualitatively and functionally distinct plexus, clearly distinguishable from the SCP and DCP. In the future, the unique qualities of the MCP identified on OCTA may further clarify middle retinal ischemic entities, such as AMN and PAMM, and may provide new insights for various ischemic pathological states including diabetic retinopathy. The development of reliable quantitative and automated software tools as well as normative databases that take into account the capillary densities in each of these networks will be important next steps.

## Supplementary Material

Refer to Web version on PubMed Central for supplementary material.

## Acknowledgments

Financial Support: This work was partially supported by NIH/NIDDK 1DP3DK108248 (AAF) and research instrument support by OptoVue, Inc. B.T.S. is a student in the Medical Scientist Training Program at Feinberg School of Medicine at Northwestern University, which is supported by T32GM008152. The funders had no role in the design or conduct of this research.

## References

1. Lipson BK, Yannuzzi LA. Complications of intravenous fluorescein injections. Int Ophthalmol Clin. 1989; 29(3):200–5. [PubMed: 2526795]
2. Weinhaus RS, Burke JM, Delori FC, Snodderly DM. Comparison of fluorescein angiography with microvascular anatomy of macaque retinas. Exp Eye Res. 1995; 61(1):1–16. [PubMed: 7556462]
3. Jia Y, Tan O, Tokayer J, et al. Split-spectrum amplitude-decorrelation angiography with optical coherence tomography. Opt Express. 2012; 20(4):4710–25. [PubMed: 22418228]

4. Chan G, Balaratnasingam C, Yu PK, et al. Quantitative morphometry of perifoveal capillary networks in the human retina. Invest Ophthalmol Vis Sci. 2012; 53(9):5502–14. [PubMed: 22815351]
5. Snodderly DM, Weinhaus RS. Retinal vasculature of the fovea of the squirrel monkey, Saimiri sciureus: three-dimensional architecture, visual screening, and relationships to the neuronal layers. J Comp Neurol. 1990; 297(1):145–63. [PubMed: 2376631]
6. Snodderly DM, Weinhaus RS, Choi JC. Neural-vascular relationships in central retina of macaque monkeys (Macaca fascicularis). J Neurosci. 1992; 12(4):1169–93. [PubMed: 1556592]
7. Henkind P. Radial peripapillary capillaries of the retina. I. Anatomy: human and comparative. Br J Ophthalmol. 1967; 51(2):115–23.
8. Provis JM. Development of the primate retinal vasculature. Prog Retin Eye Res. 2001; 20(6):799–821. [PubMed: 11587918]
9. Usui Y, Westenskow PD, Kurihara T, et al. Neurovascular crosstalk between interneurons and capillaries is required for vision. J Clin Invest. 2015; 125(6):2335–46. [PubMed: 25915585]
10. Arend O, Wolf S, Jung F, et al. Retinal microcirculation in patients with diabetes mellitus: dynamic and morphological analysis of perifoveal capillary network. Br J Ophthalmol. 1991; 75(9):514–8. [PubMed: 1911651]
11. Ishibazawa A, Nagaoka T, Takahashi A, et al. Optical Coherence Tomography Angiography in Diabetic Retinopathy: A Prospective Pilot Study. Am J Ophthalmol. 2015; 160(1):35–44. [PubMed: 25896459]
12. Sun JK, Lin MM, Lammer J, et al. Disorganization of the retinal inner layers as a predictor of visual acuity in eyes with center-involved diabetic macular edema. JAMA Ophthalmol. 2014; 132(11):1309–16. [PubMed: 25058813]
13. Chen X, Rahimy E, Sergott RC, et al. Spectrum of Retinal Vascular Diseases Associated With Paracentral Acute Middle Maculopathy. Am J Ophthalmol. 2015; 160(1):26–34.e1. [PubMed: 25849522]
14. Scarinci F, Jampol LM, Linsenmeier RA, Fawzi AA. Association of Diabetic Macular Nonperfusion With Outer Retinal Disruption on Optical Coherence Tomography. JAMA Ophthalmol. 2015; 133(9):1036–44. [PubMed: 26158562]
15. Tan PE, Yu PK, Balaratnasingam C, et al. Quantitative confocal imaging of the retinal microvasculature in the human retina. Invest Ophthalmol Vis Sci. 2012; 53(9):5728–36. [PubMed: 22836777]
16. Spaide RF, Fujimoto JG, Waheed NK. IMAGE ARTIFACTS IN OPTICAL COHERENCE TOMOGRAPHY ANGIOGRAPHY. Retina. 2015; 35(11):2163–80. [PubMed: 26428607]
17. Jia Y, Bailey ST, Hwang TS, et al. Quantitative optical coherence tomography angiography of vascular abnormalities in the living human eye. Proc Natl Acad Sci U S A. 2015; 112(18):E2395–402. [PubMed: 25897021]
18. Toussaint D, Kuwabara T, Cogan DG. Retinal vascular patterns. II. Human retinal vessels studied in three dimensions. Arch Ophthalmol. 1961; 65:575–81.
19. Savastano MC, Lumbroso B, Rispoli M. IN VIVO CHARACTERIZATION OF RETINAL VASCULARIZATION MORPHOLOGY USING OPTICAL COHERENCE TOMOGRAPHY ANGIOGRAPHY. Retina. 2015; 35(11):2196–203. [PubMed: 25932558]
20. Bonnin S, Mane V, Couturier A, et al. NEW INSIGHT INTO THE MACULAR DEEP VASCULAR PLEXUS IMAGED BY OPTICAL COHERENCE TOMOGRAPHY ANGIOGRAPHY. Retina. 2015; 35(11):2347–52. [PubMed: 26469532]
21. Genevois O, Paques M, Simonutti M, et al. Microvascular remodeling after occlusion-recanalization of a branch retinal vein in rats. Invest Ophthalmol Vis Sci. 2004; 45(2):594–600. [PubMed: 14744903]
22. Gariano RF, Iruela-Arispe ML, Hendrickson AE. Vascular development in primate retina: comparison of laminar plexus formation in monkey and human. Invest Ophthalmol Vis Sci. 1994; 35(9):3442–55. [PubMed: 8056520]
23. Samara WA, Say EA, Khoo CT, et al. CORRELATION OF FOVEAL AVASCULAR ZONE SIZE WITH FOVEAL MORPHOLOGY IN NORMAL EYES USING OPTICAL COHERENCE TOMOGRAPHY ANGIOGRAPHY. Retina. 2015; 35(11):2188–95. [PubMed: 26469536]

24. Couturier A, Mane V, Bonnin S, et al. CAPILLARY PLEXUS ANOMALIES IN DIABETIC RETINOPATHY ON OPTICAL COHERENCE TOMOGRAPHY ANGIOGRAPHY. Retina. 2015; 35(11):2384–91. [PubMed: 26469531]
25. Takase N, Nozaki M, Kato A, et al. ENLARGEMENT OF FOVEAL AVASCULAR ZONE IN DIABETIC EYES EVALUATED BY EN FACE OPTICAL COHERENCE TOMOGRAPHY ANGIOGRAPHY. Retina. 2015; 35(11):2377–83. [PubMed: 26457396]
26. Caprara C, Thiersch M, Lange C, et al. HIF1A is essential for the development of the intermediate plexus of the retinal vasculature. Invest Ophthalmol Vis Sci. 2011; 52(5):2109–17. [PubMed: 21212189]
27. Moore J, Bagley S, Ireland G, et al. Three dimensional analysis of microaneurysms in the human diabetic retina. J Anat. 1999; 194(Pt 1):89–100. [PubMed: 10227670]
28. Horii T, Murakami T, Nishijima K, et al. Optical coherence tomographic characteristics of microaneurysms in diabetic retinopathy. Am J Ophthalmol. 2010; 150(6):840–8. [PubMed: 20855054]
29. Wang H, Chhablani J, Freeman WR, et al. Characterization of diabetic microaneurysms by simultaneous fluorescein angiography and spectral-domain optical coherence tomography. Am J Ophthalmol. 2012; 153(5):861–7.e1. [PubMed: 22300473]
30. Tan PE, Yu PK, Cringle SJ, Yu DY. Quantitative assessment of the human retinal microvasculature with or without vascular comorbidity. Invest Ophthalmol Vis Sci. 2014; 55(12):8439–52. [PubMed: 25425309]
31. Bos PJ, Deutman AF. Acute macular neuroretinopathy. Am J Ophthalmol. 1975; 80(4):573–84. [PubMed: 1180301]
32. Fawzi AA, Pappuru RR, Sarraf D, et al. Acute macular neuroretinopathy: long-term insights revealed by multimodal imaging. Retina. 2012; 32(8):1500–13. [PubMed: 22846801]
33. Munk MR, Jampol LM, Cunha Souza E, et al. New associations of classic acute macular neuroretinopathy. Br J Ophthalmol. 2015
34. Sarraf D, Rahimy E, Fawzi AA, et al. Paracentral acute middle maculopathy: a new variant of acute macular neuroretinopathy associated with retinal capillary ischemia. JAMA Ophthalmol. 2013; 131(10):1275–87. [PubMed: 23929382]
35. Rahimy E, Kuehlewein L, Sadda SR, Sarraf D. Paracentral Acute Middle Maculopathy: What We Knew Then and What We Know Now. Retina. 2015; 35(10):1921–30. [PubMed: 26360227]
36. Dansingani KK, Inoue M, Engelbert M, Freund KB. Optical coherence tomographic angiography shows reduced deep capillary flow in paracentral acute middle maculopathy. Eye (Lond). 2015

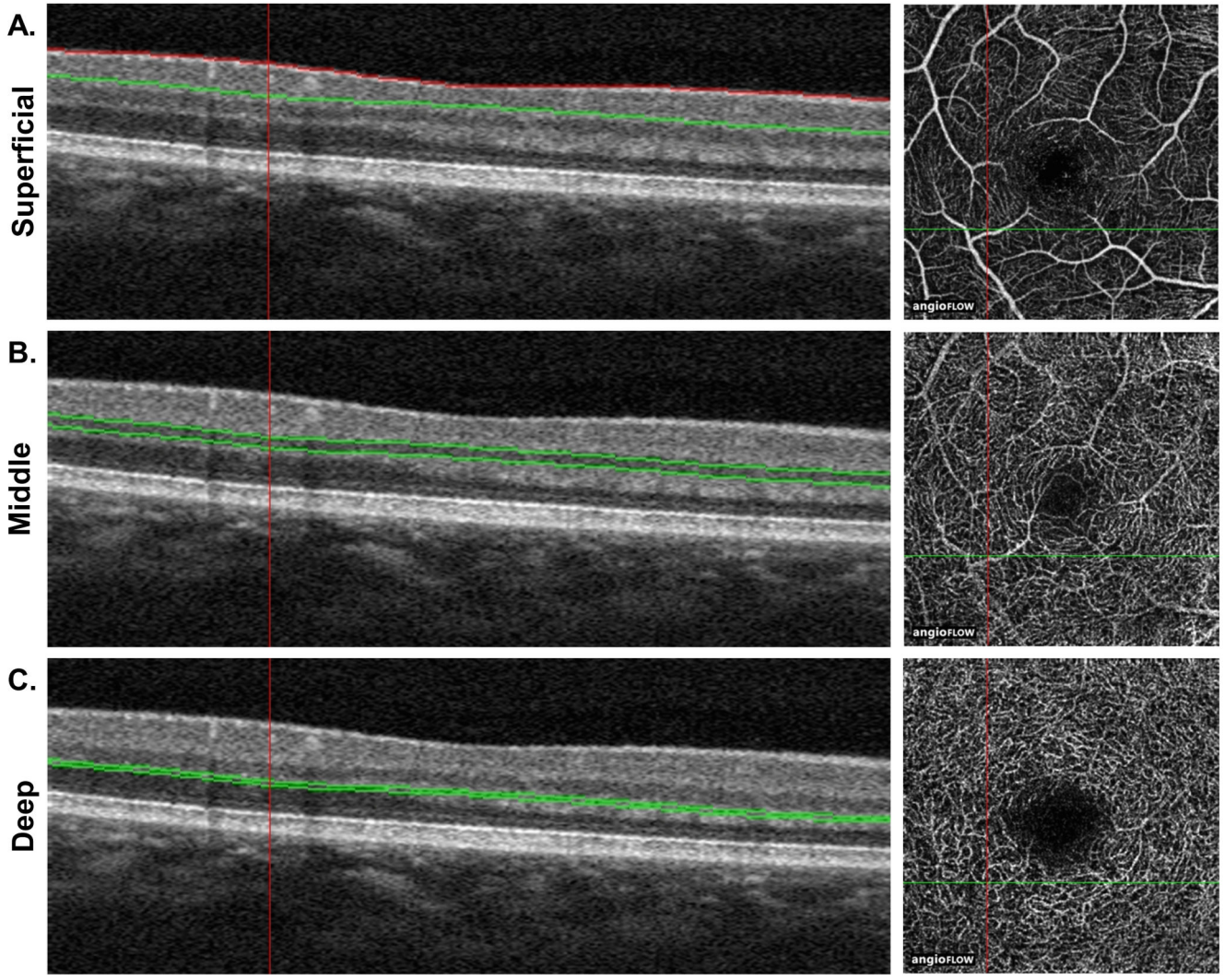


**Figure 1. Optical coherence tomography angiography (OCTA) segmentation used to visualize the three capillary plexuses in Method 3**

**A.** The superficial capillary plexus (SCP) boundaries encompass the nerve fiber layer (NFL), ganglion cell layer (GCL) and inner plexiform layer (IPL). The inner boundary was set at 3 μm beneath the internal limiting membrane (ILM), and the outer boundary was set at a 25 μm offset from the IPL. **B.** The middle capillary plexus (MCP) was captured with a 30 μm band to encompass the inner nuclear layer (INL). The inner boundary was set at 0 μm beneath the IPL and the outer boundary was set at 30 μm below the IPL. **C.** The deep capillary plexus (DCP) was set by using a 15 μm band set on the outer plexiform layer (OPL). The inner boundary was set at 45 μm beneath the IPL and the outer boundary was set at 60 μm beneath the IPL.

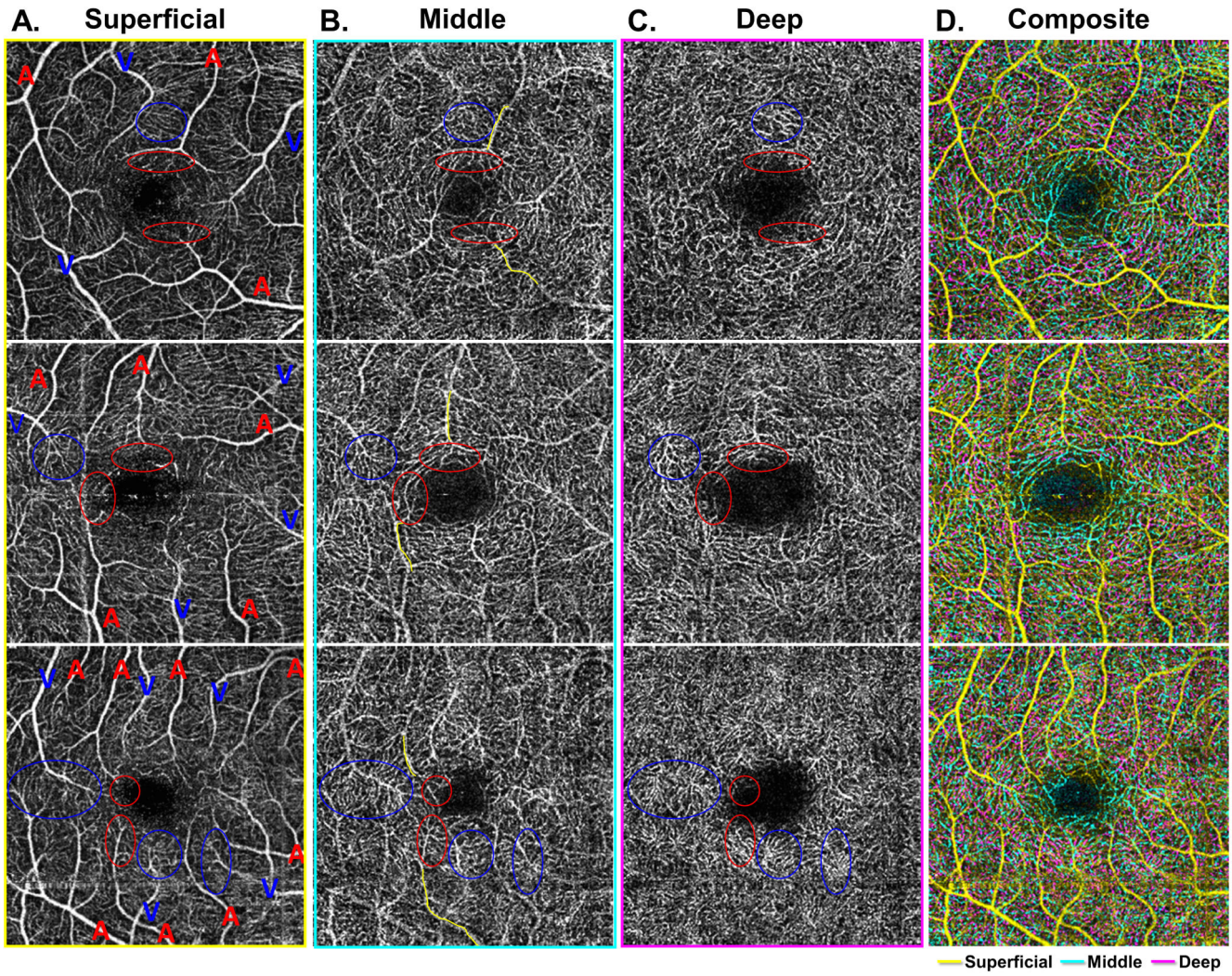


**Figure 2. Characterization of arteriolar and venular branching patterns at the level of the three capillary plexuses**

A-C: Demonstrate the three capillary plexuses of three different eyes from healthy control patients (each row). Arterioles and venules are labeled with a red A or blue V, respectively, in the superficial capillary plexus (SCP) (Column A), with points of interest circled in red for arterioles and blue for venules in each image. In the middle capillary plexus (MCP) (Column B), outlines of arterioles from the SCP are partially outlined with yellow. In these images, arterioles can be seen to give off unique branches in the MCP that are distinct from the deep capillary plexus (DCP) (Column C). Venules give off distinct vortices best seen in the DCP. The composite image (Column D) shows an overlay of all three capillary plexus layers, with the SCP in yellow, MCP in cyan, and DCP in magenta.

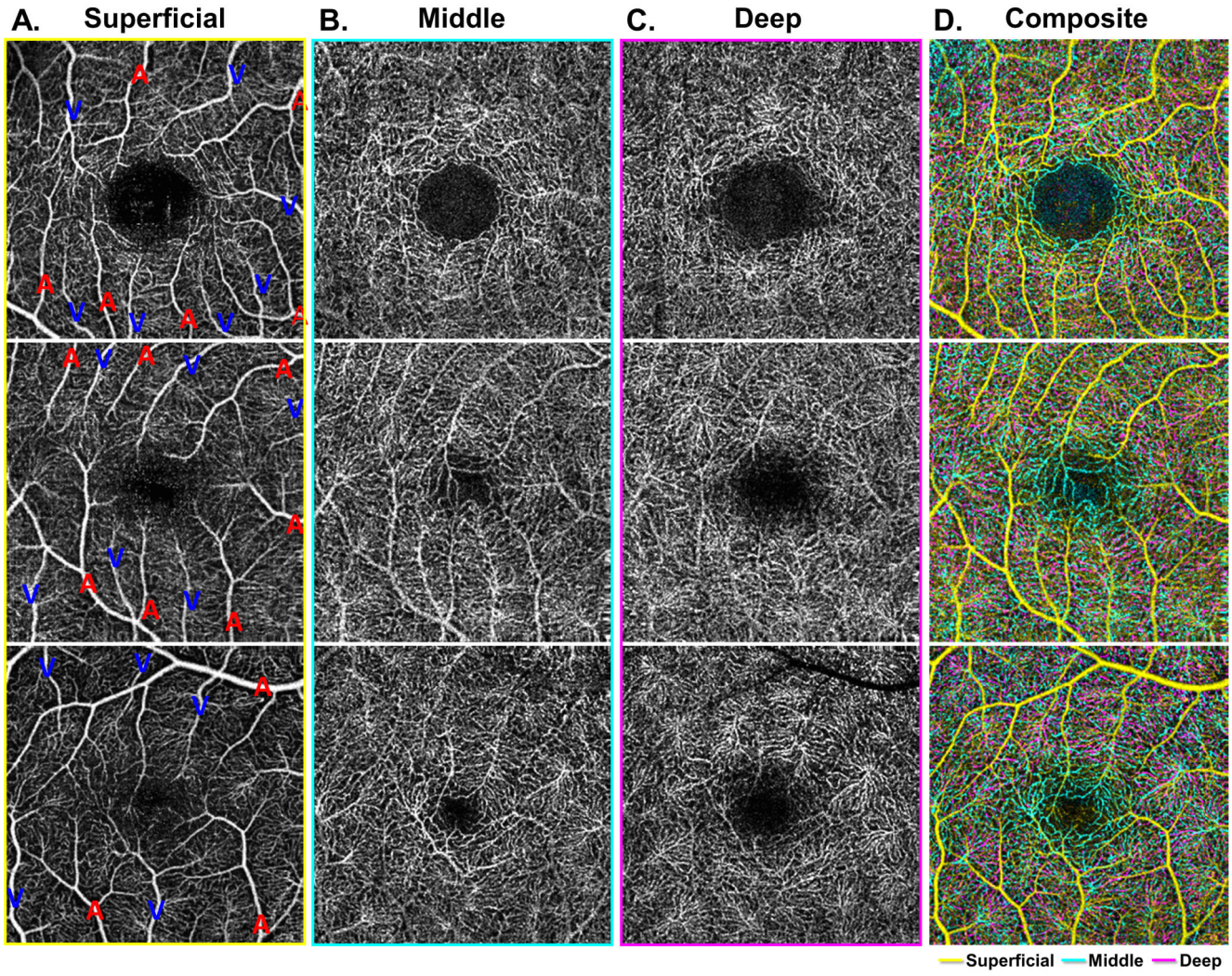


**Figure 3. Characterization of the foveal avascular zone (FAZ) at the level of the three capillary plexuses**

A-C: Demonstrate the three capillary plexuses of three different eyes from healthy control patients (each row). Arterioles and veins are labeled with a red A or blue V, respectively, in the superficial capillary plexus (SCP) (Column A). In the middle capillary plexus (MCP) (Column B), the border of the foveal avascular zone (FAZ) is best observed as a well-demarcated and clearly circumscribed area, with a border that is composed of branches from both arterioles and venules in the MCP. This regular FAZ border is not observed in the deep capillary plexus (DCP) (Column C). The composite image (Column D) shows an overlay of all three capillary plexus layers, with the SCP in yellow, MCP in cyan, and DCP in magenta. In the composite image, there is significant overlap between the capillary networks, but a distinct area of cyan is observed in the FAZ region, while the magenta DCP does not approach the FAZ region to the same extent. Consequently, the FAZ is appreciably larger in the DCP compared to the MCP.

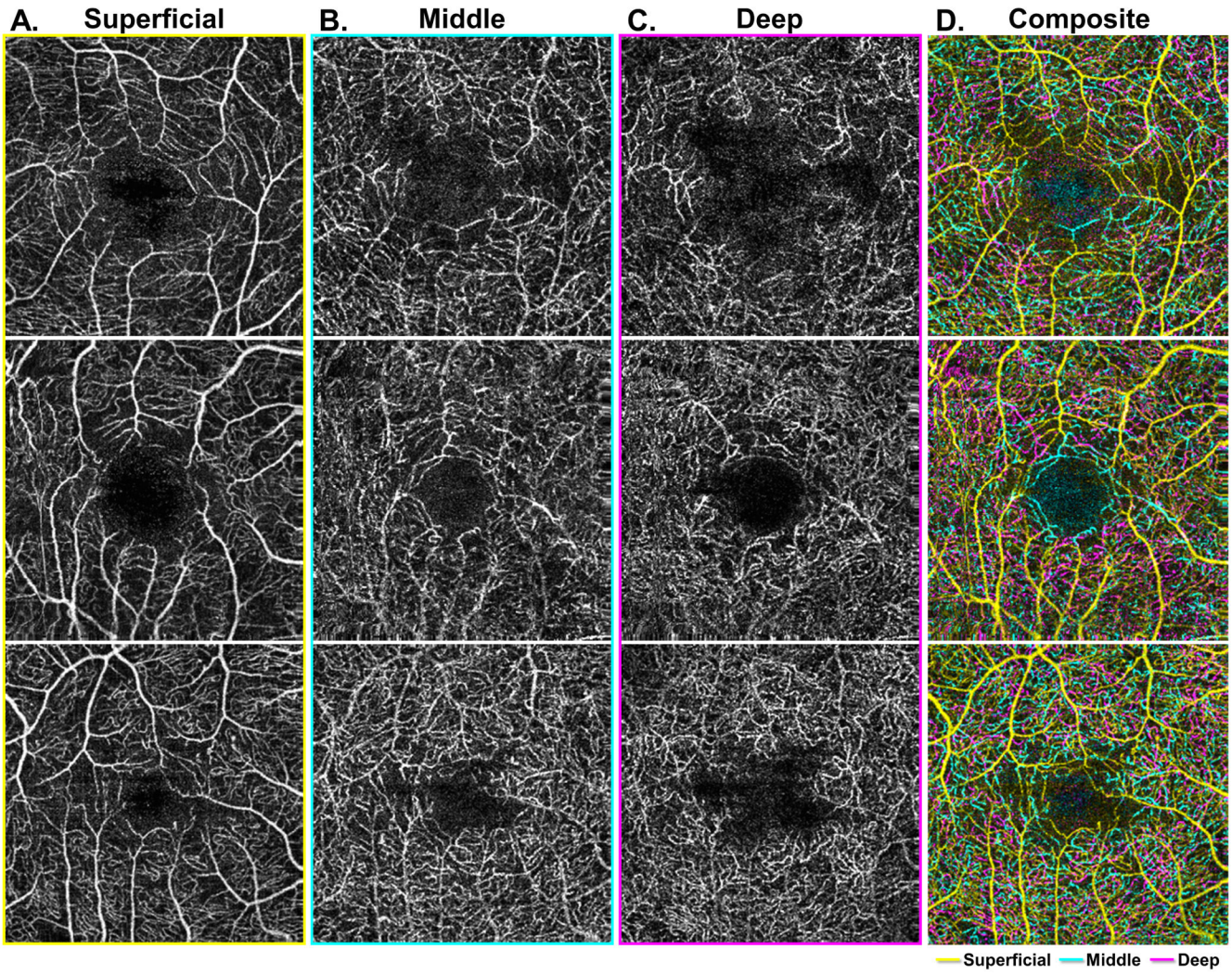


**Figure 4. Characterization of capillary non-perfusion and FAZ boundaries at the level of the three capillary plexuses**

A-C: Demonstrate the three capillary plexuses of three different eyes from diabetic patients (each row). The three different capillary plexuses show consistently different areas of non-perfusion, including different shapes and extent of the foveal avascular zone (FAZ). When compared to the middle capillary plexus (MCP) (Column B), the FAZ of the deep capillary plexus (DCP) extends to cover a broader area. Furthermore, the well-demarcated border of the FAZ in the MCP seen in healthy control eyes is compromised with loss border integrity in diabetic eyes, evidenced by multiple breaks and gaps observable in the FAZ border of diabetic eyes in the MCP. The composite image (Column D) shows an overlay of all three capillary plexus layers, with the superficial capillary plexus (SCP) in yellow, MCP in cyan, and DCP in magenta. In the composite images, there is noticeably less overlap between the capillary networks as observed in healthy control eyes.

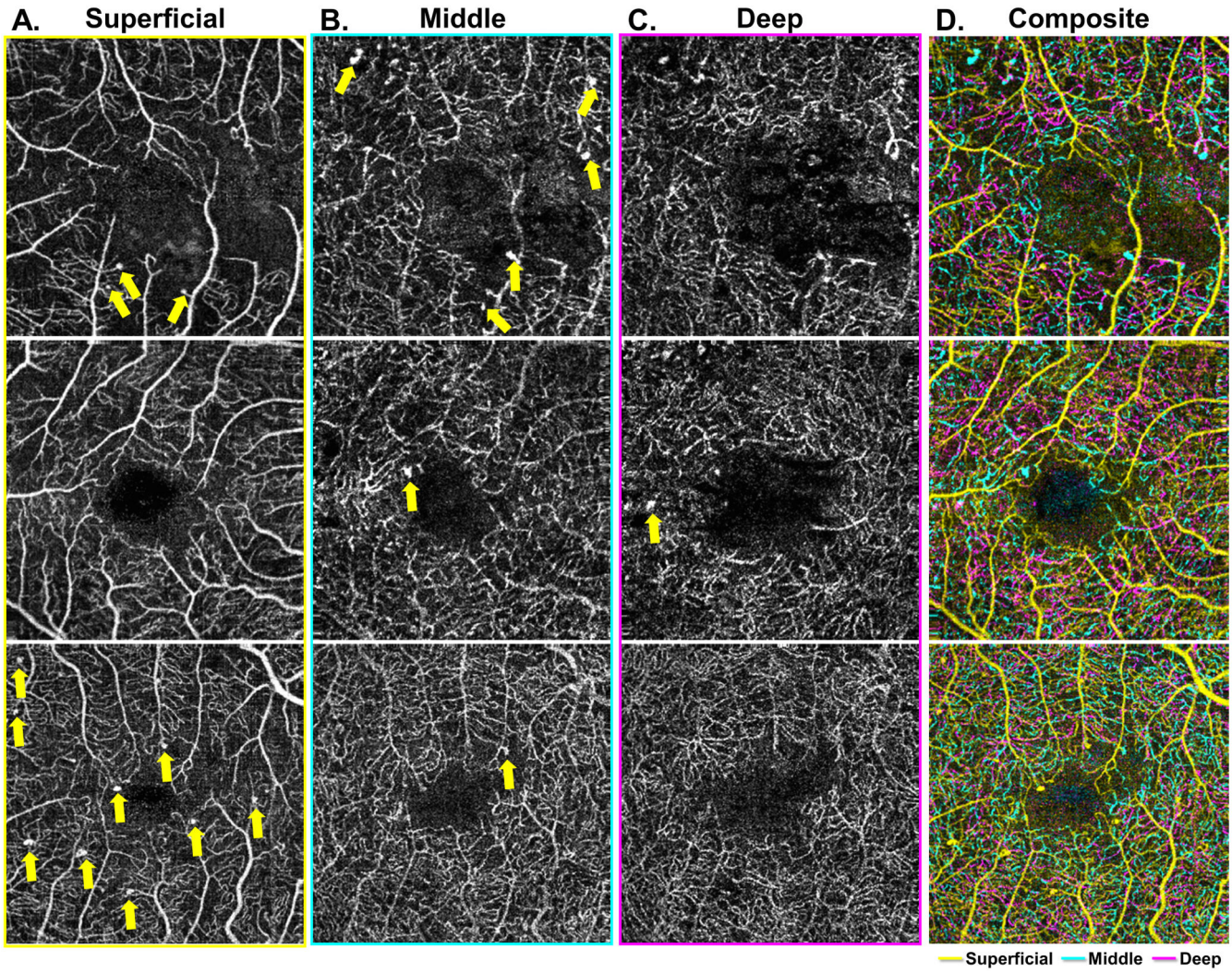


**Figure 5. Characterization of microaneurysm distribution at the level of the three capillary plexuses**

A-C: Demonstrate the three capillary plexuses of three different eyes from diabetic patients (each row). Microaneurysms are identified and labeled in each of the three capillary plexuses. The composite image (Column D) shows an overlay of all three capillary plexus layers, with the superficial capillary plexus (SCP) in yellow, the middle capillary plexus (MCP) in cyan, and the deep capillary plexus (DCP) in magenta. Columns A and B show multiple microaneurysms in both the SCP and MCP layers respectively, identified by yellow arrows. Column C shows an example of a microaneurysm arising in the in the DCP.

**Table 1**

MORPHOLOGICAL CHARACTERISTICS OF THE THREE CAPILLARY PLEXUSES IN HEALTHY AND DIABETIC EYES

| | HEALTHY CONTROL EYES | DIABETIC EYES |
|---|---|---|
| **Superficial Capillary Plexus** | • Arterioles with wider capillary-free zone | |
| **Middle Capillary Plexus** | • Distinct branches from arterioles<br>• Well-demarcated foveal avascular zone with capillary border containing contributions arising from both arterioles and venules<br>• Foveal avascular zone is qualitatively smallest at this level | • Loss of border integrity demarcating the foveal avascular zone |
| **Deep Capillary Plexus** | • Prominent spider-web like channels arising from venules<br>• Larger and less well-defined foveal avascular zone | • Enlargement of the foveal avascular zone |
| **General Observations** | • Dense overlapping network in pseudo-color map, with significant interconnectivity between the 3 networks | • Zones of of single capillary plexus perfusion. These are better visualized in pseudocolor maps as retinal areas with non-overlapping single color vessels.<br>• Non-overlapping zones of non-perfusion<br>• Varying shapes and extent of the foveal avascular zone<br>• Microaneurysms observed in all three plexus layers |

*Retina*. Author manuscript; available in PMC 2017 November 01.